

Regge trajectories for the doubly heavy diquarks

Xia Feng,^{1,*} Jiao-Kai Chen,^{1,†} and Jia-Qi Xie^{1,‡}

¹*School of Physics and Information Engineering,
Shanxi Normal University, Taiyuan 030031, China*

(Dated: August 28, 2023)

The concept of diquark is important for understanding hadron structure and high-energy particle reactions. We attempt to apply the Regge trajectory approach to the doubly heavy diquarks. We present a method for determining the parameters in the diquark Regge trajectory. The spectra of diquarks (cc), (bb), and (bc) are obtained by using the Regge trajectory approach and are found to agree with other theoretical results. The diquark Regge trajectory becomes a new and very simple approach for estimating the spectra of diquarks.

Keywords: Regge trajectory, diquark, spectra

I. INTRODUCTION

The concept of diquark is important for understanding hadron structure and high-energy particle reactions [1–8]. In the diquark picture, baryons are bound states of a diquark and one quark [2, 9]. A tetraquark is composed of a diquark and an antidiquark [10–12]. Pentaquarks are clusters of two diquarks and one antiquark [8, 10, 11] or of one diquark and one triquark [13]. Phenomenology suggests that diquark correlations might play a material role in the formation of exotic tetraquarks and pentaquarks [8, 10, 11, 14, 15]. Diquark substructure affects the static properties of baryons, tetraquarks and pentaquarks.

Various authors have studied the spectra of diquarks. In Ref. [16], the spectra of the doubly heavy diquarks (QQ') are calculated by using the Schrödinger equation. In Ref. [17], the mass spectra of the doubly heavy diquarks are obtained by the quasipotential equation of the Schrödinger type. In Ref. [18], the masses of different kinds of diquarks are calculated within a nonrelativistic potential model. In Refs. [19–25], the spectra of diquarks are computed by using the Bethe-Salpeter equation. In Refs. [26, 27], the diquark masses are calculated by the spinless Salpeter equation. In Ref. [28], the diquark masses are obtained from lattice QCD.

The Regge trajectory is one of the effective approaches for studying hadron spectra [29–55]. In the present work, we attempt to apply this approach to investigate the diquark spectra, even though diquarks are colored states and not physical [8]. We use the term diquark Regge trajectory following the same nomenclature as the hadron Regge trajectory [56]. Our focus in this work is on the doubly heavy diquarks (cc), (bb) and (bc).

The paper is organized as follows: In Sec. II, the Regge trajectory relation is obtained from the quadratic form of the spinless Salpeter-type equation (QSSE). In Sec. III, we investigate the Regge trajectories for the doubly

heavy diquarks. The conclusions are presented in Sec. IV.

II. REGGE TRAJECTORY RELATIONS

We apply the ansatz [52] to describe the diquark spectra

$$M = \beta_x(x + c_{0x})^\nu + m_R, \quad (x = l, n_r) \quad (1)$$

where M is the diquark mass, l is the orbital angular momentum and n_r is the radial quantum number. β_x , ν and m_R can be determined by employing the QSSE, see Eq. (10). c_0 varies with different trajectories.

A. QSSE

The QSSE reads as [57–65]

$$M^2\Psi(\mathbf{r}) = M_0^2\Psi(\mathbf{r}) + \mathcal{U}\Psi(\mathbf{r}), \quad M_0 = \omega_1 + \omega_2, \quad (2)$$

where Ψ is the diquark wave function, ω_1 and ω_2 are the square-root operators of the relativistic kinetic energy of quark q and quark q' , respectively,

$$\omega_i = \sqrt{m_i^2 + \mathbf{p}^2} = \sqrt{m_i^2 - \Delta}, \quad (3)$$

$$\mathcal{U} = M_0 V_{qq'} + V_{qq'} M_0 + V_{qq'}^2. \quad (4)$$

m_1 and m_2 are the effective masses of quark q and quark q' , respectively. In $SU_c(3)$, there is attraction between quark pairs (qq') in the color antitriplet channel, and this is just twice weaker than in the color singlet $q\bar{q}'$ in the one-gluon exchange approximation [11]. Only the $\bar{3}_c$ representation of $SU_c(3)$ is considered in the present work and the 6_c representation [66, 67] is not considered. In the case of diquarks in a color $\bar{3}_c$ state, the relation [16, 17]

$$V_{qq'} = \frac{V_{q\bar{q}'}}{2} \quad (5)$$

*Electronic address: sxsdwxfx@163.com

†Electronic address: chenjk@sxnu.edu.cn, chenjkphy@outlook.com

‡Electronic address: 1462718751@qq.com

is used for the quark-quark interaction. The quark-antiquark interaction in the mesons adopts the Cornell potential [68],

$$V_{q\bar{q}'}(r) = -\frac{\alpha}{r} + \sigma r + C, \quad (6)$$

where the first term is the color Coulomb potential parameterized by the coupling strength α . The second term is the linear confining potential, and σ is the string tension. C is a fundamental parameter [69, 70].

B. Regge trajectories obtained from the QSSE

For the heavy-heavy diquarks, $m_1, m_2 \gg |\mathbf{p}|$, Eq. (2) reduces to

$$M^2 \Psi(\mathbf{r}) = \left[(m_1 + m_2)^2 + \frac{m_1 + m_2}{\mu} \mathbf{p}^2 \right] \Psi(\mathbf{r}) + 2(m_1 + m_2)V\Psi(\mathbf{r}), \quad (7)$$

where

$$\mu = m_1 m_2 / (m_1 + m_2). \quad (8)$$

By employing the Bohr-Sommerfeld quantization approach [71, 72] and using Eqs. (6) and (7), we can obtain the orbital and radial Regge trajectories [62, 65],

$$M^2 \sim 3(m_1 + m_2) \left(\frac{\sigma'^2}{\mu} \right)^{1/3} l^{2/3} \quad (l \gg n_r),$$

$$M^2 \sim (3\pi)^{2/3} (m_1 + m_2) \left(\frac{\sigma'^2}{\mu} \right)^{1/3} n_r^{2/3} \quad (n_r \gg l), \quad (9)$$

where $\sigma' = \sigma/2$. By considering the constant term of m_1 and m_2 , as well as the omitted term proportional to $n_r^{4/3}$, we can obtain (1) from Eq. (9) with the following parameters [52]

$$\nu = 2/3, \quad \beta_x = c_{fx} c_x c_c, \quad m_R = m_1 + m_2 + \epsilon_c. \quad (10)$$

Here, ϵ_c is a constant which is a part of the interaction energy. Usually, $\epsilon_c = C/2$ where C is given by Eq. (6). The constants c_x and c_c are

$$c_c = \left(\frac{\sigma'^2}{\mu} \right)^{1/3}, \quad c_l = \frac{3}{2}, \quad c_{n_r} = \frac{(3\pi)^{2/3}}{2}. \quad (11)$$

Both c_{fl} and c_{fn_r} are theoretically equal to 1 and are fitted in practice. In Eqs. (10) and (11), $m_1, m_2, \epsilon_c, c_x, c_{fx}$ and σ' are universal for the heavy-heavy diquarks. c_{0x} is determined by fitting a given Regge trajectory. The simple formula (1) with (10) and (11) can give results which are consistent with other theoretical predictions; see Sec. III.

If the confining potential is $V_{qq'}(r) = \sigma' r^a$ ($a > 0$), Eq. (1) becomes

$$M = m_R + c_{fx} c_x c_c (x + c_{0x})^{2a/(a+2)}. \quad (12)$$

c_x and c_c are

$$c_l = \left(1 + \frac{a}{2} \right) \left(\frac{1}{a} \right)^{a/(a+2)},$$

$$c_{n_r} = \left(\frac{1}{2} \right)^{a/(a+2)} \left(\frac{a\pi}{B(1/a, 3/2)} \right)^{2a/(a+2)},$$

$$c_c = \left(\frac{\sigma'^2}{\mu^a} \right)^{1/(a+2)}, \quad (13)$$

where $B(x, y)$ denotes the beta function [73]. Different forms of kinematic terms corresponding to different energy regions will yield different behaviors of the Regge trajectories [52, 65]. \mathbf{p} and r^a lead to $M \sim x^{a/(a+1)}$ while \mathbf{p}^2 and r^a result in $M \sim x^{2a/(a+2)}$ ($x = l, n_r$). For the heavy-heavy systems, the Regge trajectories plotted in the (M, x) plane will exhibit an upward convexity if $a > 2$, a linear relationship if $a = 2$, and a downward concavity if $a < 2$.

Equation (1) with (10) can lead to another form of the Regge trajectory [52, 54, 56]

$$(M - m_R)^2 = \alpha_x (x + c_{0x})^{4/3} \quad (x = l, n_r), \quad (14)$$

where $\alpha_x = c_{fx}^2 c_x^2 c_c^2$. Equation (14) is similar to the formulas in Refs. [48, 50]. For the confining potential $V_{qq'}(r) = \sigma' r^a$ ($a > 0$), Eq. (14) becomes

$$(M - m_R)^2 = \alpha_x (x + c_{0x})^{4a/(a+2)}. \quad (15)$$

For the heavy-heavy systems, the Regge trajectories plotted in the $((M - m_R)^2, x)$ plane will be convex upwards if $a > 2/3$, be linear if $a = 2/3$, and be concave downwards if $a < 2/3$ [63].

III. REGGE TRAJECTORIES FOR THE DOUBLY HEAVY DIQUARKS

In this section, the Regge trajectories for the doubly heavy diquarks (cc), (bb) and (bc) are investigated by using Eq. (1).

A. Preliminary

The state of diquark (qq') is denoted as $[qq']_{n^{2s+1}l_j}^{\bar{3}_c}$ or $\{qq'\}_{n^{2s+1}l_j}^{\bar{3}_c}$, where $\{qq'\}$ and $[qq']$ indicate the permutation symmetric and antisymmetric flavor wave functions, respectively. $n = n_r + 1$, $n_r = 0, 1, \dots$, where n_r is the radial quantum number. s is the total spin of two quarks, l is the orbital quantum number, and j is the spin of the diquark (qq'). $\bar{3}_c$ denotes the color antitriplet state of diquark.

For the diquarks (cc) and (bb), the states with antisymmetric flavor wave function do not exist. For the diquark (bc), both $[bc]$ and $\{bc\}$ exist; see the Appendix and Table IX for more discussions.

Using the formula (1) with (10) and (11) [$\sigma' = \sigma$ and $\epsilon_c = C$ for mesons] and the PDG averaged masses from the Particle Data Group [74], we fit the radial and orbital Regge trajectories for the charmonia, bottomonia and the bottom-charmed mesons, respectively. The quality of a fit is measured by the quantity χ^2 defined by [75]

$$\chi^2 = \frac{1}{N-1} \sum_{i=1}^N \left(\frac{M_{fi} - M_{ei}}{M_{ei}} \right)^2, \quad (16)$$

where N is the number of points on the trajectory, M_{fi} is fitted value and M_{ei} is the experimental value or the theoretical value of the i -th particle. The parameters are determined by minimizing χ^2 . We use the following parameter values [17, 76] to fit the Regge trajectories for the doubly heavy diquarks,

$$\begin{aligned} m_b &= 4.88 \text{ GeV}, & m_c &= 1.55 \text{ GeV}, \\ \sigma &= 0.18 \text{ GeV}^2, & C &= -0.30 \text{ GeV}, \\ c_{fl} &= 1.17, & c_{fn_r} &= 1. \end{aligned} \quad (17)$$

The values of m_b , m_c , σ and C are taken directly from [17, 76]. c_{fl} and c_{fn_r} are obtained by fitting the Regge trajectories for the doubly heavy mesons. These parameters are universal for all doubly heavy diquark Regge trajectories. There is only one free parameter c_{0x} in (1) or (14), which is determined by fitting the corresponding meson Regge trajectories and varies with different diquark Regge trajectories. There is not compelling reason why c_{0x} obtained by fitting the meson Regge trajectories can be used directly to calculate the diquark Regge trajectories. We use this method as a provisional method to determine c_{0x} before finding a better one. It validates this method that the fitted results for the diquarks (cc), (bb), and (bc) agree with the theoretical values obtained by using other approaches, see the discussions in the following subsections.

B. Regge trajectories for the (cc) diquark

By using Eq. (1) with (10), (11) and (17) [$\sigma' = \sigma$ and $\epsilon_c = C$ for mesons] to fit the radial $J/\psi(1S)$ and $h_c(1P)$ Regge trajectories, we have $c_{0n_r} = 0.205$ and $c_{0n_r} = 0.907$, respectively. Fitting the orbital $\eta_c(1S)$ and $J/\psi(1S)$ Regge trajectories gives $c_{0l} = 0.188$ and $c_{0l} = 0.337$, respectively. To calculate the masses of the $\{cc\}_{1^3d_1}^{\bar{3}_c}$ and $\{cc\}_{1^3d_2}^{\bar{3}_c}$ states, we fit the orbital $\chi_{c0}(1P)$ and $\chi_{c1}(1P)$ Regge trajectories and obtain $c_{0l} = 1.016$, $c_{0l} = 1.231$, respectively.

Substituting the values in Eq. (17) and the obtained c_{0x} into (10) and (11), Eq. (1) is determined [$\sigma' = \sigma/2$ and $\epsilon_c = C/2$ for diquarks]. We use (1) to calculate the masses of diquark (cc), which are listed in Tables I, II and VII. As we fit the parameter c_{0x} , the spin-dependent effects are considered in fact. For example, we fit the orbital $J/\psi(1S)$ Regge trajectory, then the obtained c_{0l}

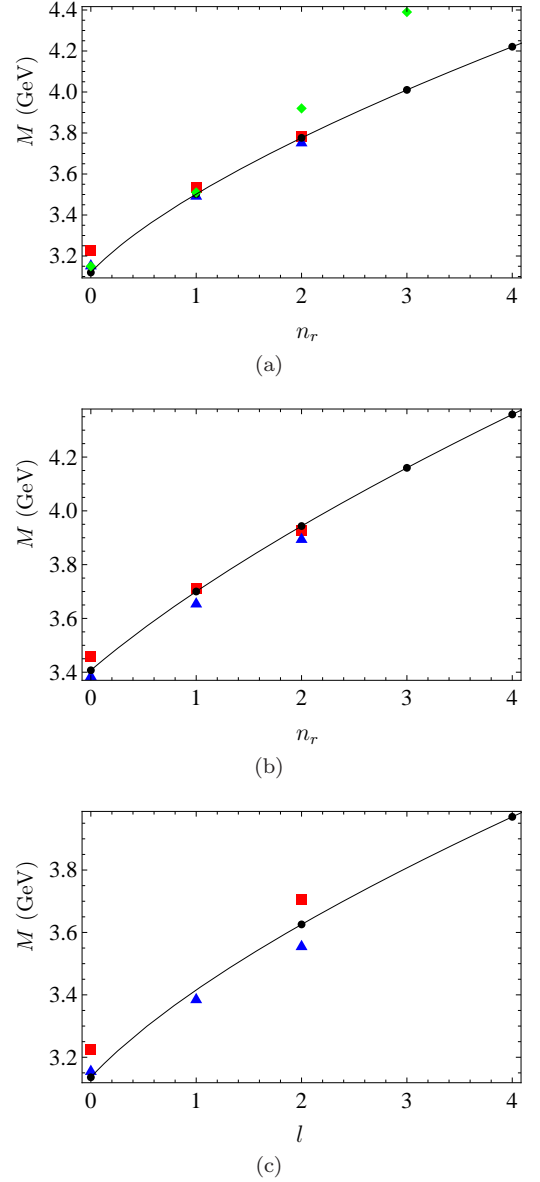


FIG. 1: The radial and orbital Regge trajectories for the (cc) diquark. (a) Radial Regge trajectory for the diquark $\{cc\}_{1^3s_1}^{\bar{3}_c}$ state. (b) Radial Regge trajectory for the diquark $\{cc\}_{1^1p_1}^{\bar{3}_c}$ state. (c) Orbital Regge trajectory for the $\{cc\}_{1^3s_1}^{\bar{3}_c}$ state. The data for the red filled squares are from EFMG or FG. The data for the blue filled triangles are from GKLO. The data for the green diamonds are from GAR. The black lines and the black dots are our results. The data are listed in Tables I and II.

is used for the orbital $\{cc\}_{1^3s_1}^{\bar{3}_c}$ Regge trajectory. Here, we do not consider the ${}^3(j-1)_j - {}^3(j+1)_j$ mixing of diquarks which is similar to the mixing of different wave states of charmonium and bottomonium [77]. The mass of state $\{cc\}_{2^3s_1}^{\bar{3}_c}$ is estimated by using the radial $\{cc\}_{1^3s_1}^{\bar{3}_c}$ Regge trajectory, $m(\{cc\}_{2^3s_1}^{\bar{3}_c}) = 3.535 \text{ GeV}$. The mass of

TABLE I: Comparison of the theoretical values (in GeV) for the diquark (cc). The data from Ref. [16] are without spin-dependent splittings. $n = n_r + 1$, $n_r = 0, 1, \dots$. n_r is the radial quantum number. s is the total spin of two quarks, l is the orbital quantum number and j is the spin of diquark. The acronyms are from the initial letters of the last name of authors.

| State ($n^{2s+1}l_j$) | EFGM [17] | GKLO [16] | GAR [18] | Our results |
|-------------------------|-----------|-----------|----------|-------------|
| 1^3s_1 | 3.226 | 3.16 | 3.15 | 3.12 |
| 2^3s_1 | 3.535 | 3.50 | 3.51 | 3.50 |
| 3^3s_1 | 3.782 | 3.76 | 3.92 | 3.78 |
| 4^3s_1 | | | 4.39 | 4.01 |
| 5^3s_1 | | | | 4.22 |
| 1^1p_1 | 3.460 | 3.39 | | 3.41 |
| 2^1p_1 | 3.712 | 3.66 | | 3.70 |
| 3^1p_1 | 3.928 | 3.90 | | 3.94 |
| 4^1p_1 | | | | 4.16 |
| 5^1p_1 | | | | 4.36 |

TABLE II: The theoretical values (in GeV) for the (cc) diquark. The data from Ref. [16] are without spin-dependent splittings. \times denotes the nonexistent states. The acronyms are from the initial letters of the last name of authors.

| State ($n^{2s+1}l_j$) | FG [76] | GKLO [16] | Our results |
|-------------------------|---------|-----------|------------------|
| 1^3s_1 | 3.226 | 3.16 | 3.14 |
| 1^3p_2 | | 3.39 | 3.42(\times) |
| 1^3d_3 | 3.704 | 3.56 | 3.63 |
| 1^3f_4 | | | 3.81(\times) |
| 1^3g_5 | | | 3.97 |

state $\{cc\}_{1^3d_1}^{\bar{3}_c}$ is computed by using the orbital $\{cc\}_{1^3p_0}^{\bar{3}_c}$ Regge trajectory, $m(\{cc\}_{1^3d_1}^{\bar{3}_c}) = 3.56$ GeV.

The spectrum from GKLO [16] is without spin-dependent splittings. The symbol \times in Table II denotes the nonexistent states according to the Pauli exclusion principle; see the Appendix for more details.

Our results obtained by the Regge trajectory approach are consistent with other theoretical results, as shown in Tables I, II, and VII and Fig. 1. As depicted in Fig. 1, our results are in agreement with EFGM [17] and GKLO[16]. The behavior of Regge trajectory is different from the data from GAR [18]; see Fig. 1(a).

C. Regge trajectories for the (bb) diquark

By using Eq. (1) in conjunction with (10), (11) and (17) to fit the radial $\Upsilon(1S)$ and $h_b(1P)$ Regge trajectories, we have $c_{0n_r} = 0.01$ and $c_{0n_r} = 0.795$, respectively. Fitting the orbital $\eta_b(1S)$ and $\Upsilon(1S)$ Regge trajectories gives $c_{0l} = 0$, $c_{0l} = 0.001$, respectively. To calculate the masses of the $\{bb\}_{1^3d_1}^{\bar{3}_c}$ and $\{bb\}_{1^3d_2}^{\bar{3}_c}$ states, we fit the orbital $\chi_{b0}(1P)$ Regge trajectory and the radial $\chi_{b1}(1P)$ Regge trajectory and obtain $c_{0l} = 0.942$, $c_{0n_r} = 0.786$, respectively.

Using Eq. (1) with (10), (11), (17) and the obtained

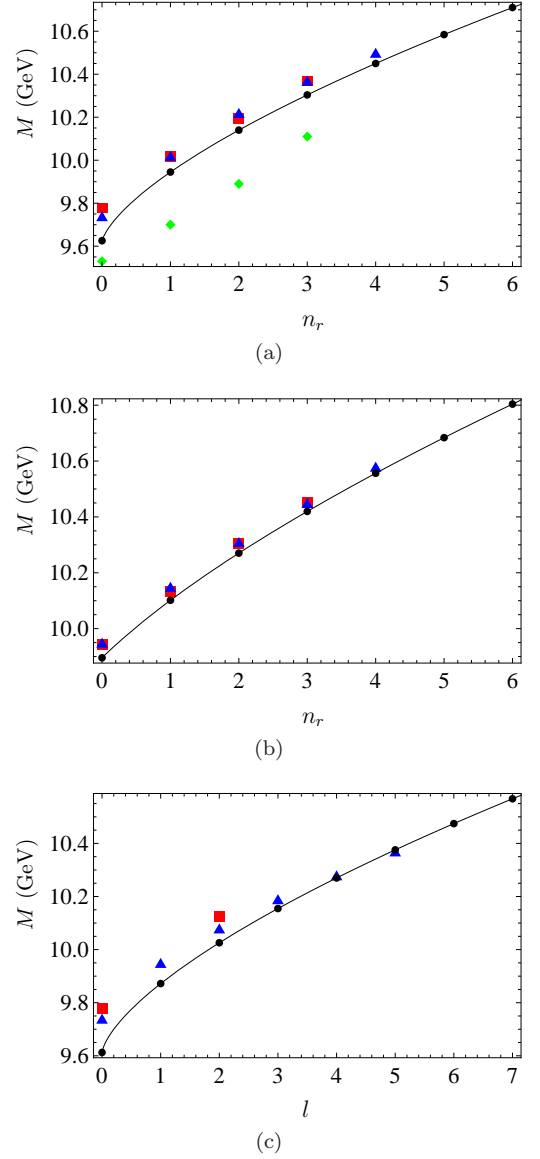


FIG. 2: The radial and orbital Regge trajectories for the (bb) diquark. (a) Radial Regge trajectory for the $\{bb\}_{1^3s_1}^{\bar{3}_c}$ state. (b) Radial Regge trajectory for the $\{bb\}_{1^3p_1}^{\bar{3}_c}$ state. (c) Orbital Regge trajectory for the $\{bb\}_{1^3s_1}^{\bar{3}_c}$ state. The data for the red filled squares are from EFGM or FG. The data for the blue filled triangles are from GKLO. The data for the green diamonds are from GAR. The black lines and the black dots are our results. The data are listed in Tables III and IV.

c_{0x} , we calculate the masses of diquark (bb). The masses are listed in Tables III, IV and VII. The corresponding Regge trajectories are in Fig. 2. As shown in Tables III, IV, and VII and Fig. 2, our results are in accordance with other theoretical results.

Similar to the (cc) diquark case, we do not consider the $^3(j-1)_j - ^3(j+1)_j$ mixing of (bb) diquarks. The mass of state $\{bb\}_{2^3s_1}^{\bar{3}_c}$ is estimated by using the radial $\{bb\}_{1^3s_1}^{\bar{3}_c}$ Regge trajectory, $m(\{bb\}_{2^3s_1}^{\bar{3}_c}) = 10.015$ GeV. The mass

of state $\{bb\}_{1^3 d_1}^{\bar{3}_c}$ is computed by using the orbital $\{bb\}_{1^3 p_0}^{\bar{3}_c}$ Regge trajectory, $m(\{bb\}_{1^3 d_1}^{\bar{3}_c}) = 10.02$ GeV.

TABLE III: Same as Table I except for the diquark (bb).

| State ($n^{2s+1}l_j$) | EFGM [17] | GAR [18] | GKLO [16] | Our results |
|-------------------------|-----------|----------|-----------|-------------|
| $1^3 s_1$ | 9.778 | 9.53 | 9.74 | 9.63 |
| $2^3 s_1$ | 10.015 | 9.70 | 10.02 | 9.95 |
| $3^3 s_1$ | 10.196 | 9.89 | 10.22 | 10.14 |
| $4^3 s_1$ | 10.369 | 10.11 | 10.37 | 10.30 |
| $5^3 s_1$ | | | 10.50 | 10.45 |
| $6^3 s_1$ | | | | 10.58 |
| $1^1 p_1$ | 9.944 | | 9.95 | 9.90 |
| $2^1 p_1$ | 10.132 | | 10.15 | 10.10 |
| $3^1 p_1$ | 10.305 | | 10.31 | 10.27 |
| $4^1 p_1$ | 10.453 | | 10.45 | 10.42 |
| $5^1 p_1$ | | | 10.58 | 10.56 |
| $6^1 p_1$ | | | | 10.68 |

TABLE IV: Same as Table II except for the diquark (bb).

| State ($n^{2s+1}l_j$) | FG [76] | GKLO [16] | Our results |
|-------------------------|---------|-----------|-------------------|
| $1^3 s_1$ | 9.778 | 9.74 | 9.61 |
| $1^3 p_2$ | | 9.95 | 9.87(\times) |
| $1^3 d_3$ | 10.123 | 10.08 | 10.03 |
| $1^3 f_4$ | | 10.19 | 10.15(\times) |
| $1^3 g_5$ | | 10.28 | 10.27 |
| $1^3 h_6$ | | 10.37 | 10.38(\times) |

D. Regge trajectories for the (bc) diquark

TABLE V: Same as Table I except for the diquark (bc).

| State ($n^{2s+1}l_j$) | GAR [18] | GKLO [16] | Our results |
|-------------------------|----------|-----------|-------------|
| $1^3 s_1$ | 6.38 | 6.48 | 6.42 |
| $2^3 s_1$ | 6.66 | 6.79 | 6.75 |
| $3^3 s_1$ | 6.97 | 7.01 | 6.99 |
| $4^3 s_1$ | 7.30 | | 7.20 |
| $5^3 s_1$ | | | 7.38 |
| $1^1 s_0$ | 6.33 | 6.48 | 6.38 |
| $2^1 s_0$ | 6.60 | 6.79 | 6.73 |
| $3^1 s_0$ | 6.92 | 7.01 | 6.98 |
| $4^1 s_0$ | 7.25 | | 7.18 |
| $5^1 s_0$ | | | 7.37 |
| $1^3 p_0$ | | 6.69 | 6.64 |
| $2^3 p_0$ | | 6.93 | 6.90 |
| $3^3 p_0$ | | 7.13 | 7.12 |
| $4^3 p_0$ | | | 7.31 |
| $5^3 p_0$ | | | 7.48 |
| $1^3 d_1$ | | 6.85 | 6.84 |
| $2^3 d_1$ | | 7.05 | 7.07 |
| $3^3 d_1$ | | | 7.26 |
| $4^3 d_1$ | | | 7.44 |
| $5^3 d_1$ | | | 7.61 |

TABLE VI: Same as Table II except for the diquark (bc).

| State ($n^{2s+1}l_j$) | GKLO [16] | Our results |
|-------------------------|-----------|-------------|
| $1^1 s_0$ | 6.48 | 6.38 |
| $1^1 p_1$ | 6.69 | 6.65 |
| $1^1 d_2$ | 6.85 | 6.84 |
| $1^1 f_3$ | 6.97 | 7.00 |
| $1^1 g_4$ | 7.09 | 7.14 |
| $1^1 h_5$ | 7.19 | 7.28 |
| $1^3 s_1$ | 6.48 | 6.41 |
| $1^3 p_2$ | 6.69 | 6.67 |
| $1^3 d_3$ | 6.85 | 6.85 |
| $1^3 f_4$ | 6.97 | 7.01 |
| $1^3 g_5$ | 7.09 | 7.16 |
| $1^3 h_6$ | 7.19 | 7.29 |

Although the excited states of the diquark (bc) are unstable under the emission of soft gluons [16], the authors provide the spectra of diquark (bc). We obtain the orbital and radial diquark (bc) Regge trajectories by fitting the corresponding B_c Regge trajectories. Simultaneously, the spectra of diquark (bc) are calculated.

There are scarce experimental data for the excited B_c mesons. For the B_c^+ and $B_c(2S)^\pm$, the masses are from [74] while the theoretically predicted masses for other states are from Ref. [78].

Because b quark and c quark are not identical, both $\{bc\}$ and $[bc]$ exist and there are more Regge trajectories for diquark (bc) than that for diquarks (cc) and (bb). By using Eq. (1) with (10), (11) and (17) to fit the radial Regge trajectories for the $B_c(1^1 S_0)$, $B_c(1^3 S_1)$, $B_c(1^3 P_0)$, $B_c(1^3 D_1)$, we have $c_{0n_r} = 0.107, 0.182, 0.783, 1.516$, respectively. Fitting the orbital Regge trajectories for the $B_c(1^1 S_0)$ and $B_c(1^3 S_1)$ gives $c_{0l} = 0.169$ and $c_{0l} = 0.257$, respectively.

Using Eq. (1) with (10), (11), (17) and the obtained c_{0x} , we calculate the masses of diquark (bc). The masses are listed in Tables V, VI and VII. The corresponding Regge trajectories are in Fig. 3. As shown in Tables V, VI, VII and Fig. 3, our results are in accordance with other theoretical results.

In the B_c meson case, there is mixing of the singlet and triplet states; for example, the P-wave states are linear combinations of $^3 P_1$ and $^1 P_1$ which can be described by $P' = ^1 P_1 \cos\theta + ^3 P_1 \sin\theta$, $P = -^1 P_1 \sin\theta + ^3 P_1 \cos\theta$ [78]. In the diquark (bc) case, there will be the $^3 l_l - ^1 l_l$ mixing via the spin-orbit interaction [17] or some other mechanism. We do not consider this kind of mixed state here.

IV. CONCLUSIONS

As shown in Sec. III, the spectra of the doubly heavy diquarks (cc), (bb), and (bc) obtained by the Regge trajectory approach agree with other theoretical results. This demonstrates that the Regge trajectory relation (1), which is appropriate for mesons, baryons and

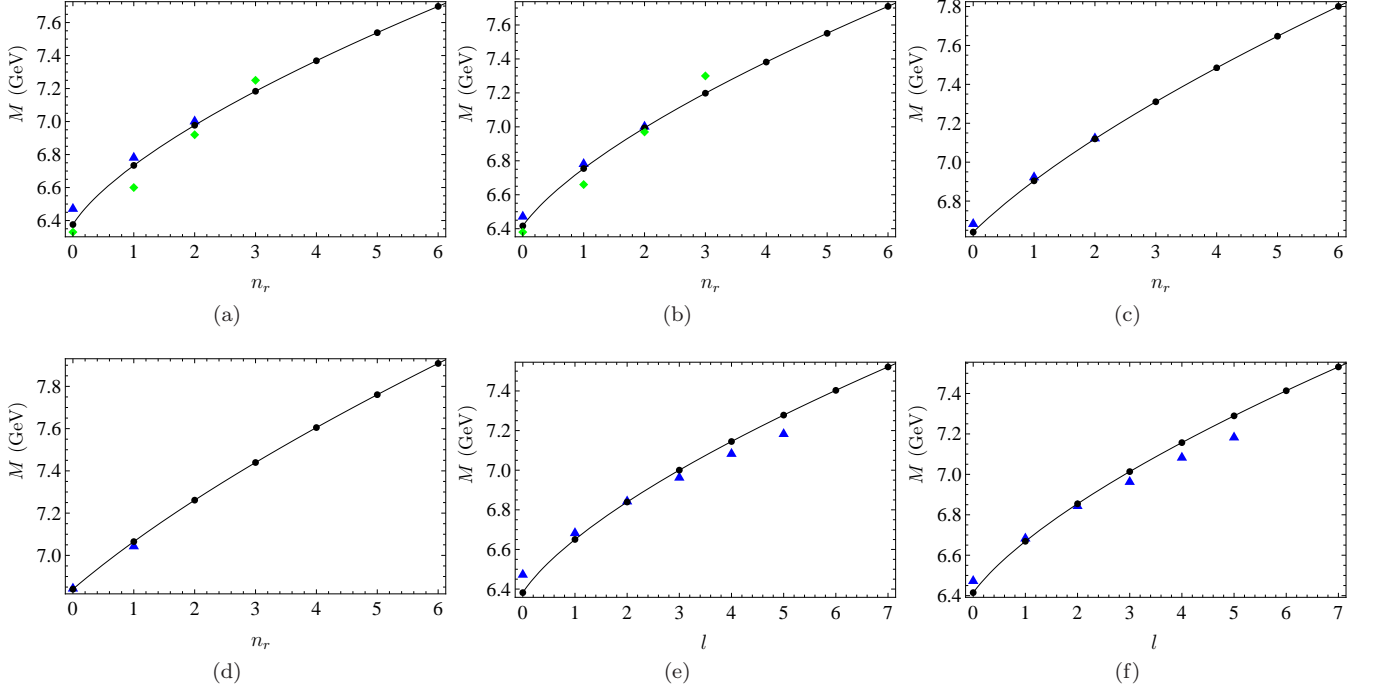


FIG. 3: The radial and orbital Regge trajectories for the (bc) diquark. (a), (b), (c) and (d) Radial Regge trajectory for the $\{bc\}_{1^3s_0}^{3c}$ state, the $\{bc\}_{1^3s_1}^{3c}$ state, the $\{bc\}_{1^3p_0}^{3c}$ and the $\{bc\}_{1^3d_1}^{3c}$ state, respectively. (e) and (f) Orbital Regge trajectory for the $\{bc\}_{1^1s_0}^{3c}$ state and the $\{bc\}_{1^1s_1}^{3c}$ state, respectively. The data for the blue filled triangles are from GKLO. The data for the green diamonds are from GAR. The black lines and the black dots are our results. The data are listed in Tables V and VI.

TABLE VII: Comparison of theoretical predictions for the masses of the doubly heavy diquarks (in GeV).

| J^P | Diquark | Our results | FG [76], FGS [79] | GKLO [16] | GPB [19] | YCRS [20] | F [27] |
|-------|------------------------|-------------|-------------------|-----------|----------|-----------|--------|
| 0^+ | $\{bc\}_{1^1s_0}^{3c}$ | 6.38 | 6.519 | 6.48 | 6.35 | 6.48 | 6.599 |
| 0^- | $\{bc\}_{1^3p_0}^{3c}$ | 6.64 | | 6.69 | 6.47 | 6.62 | |
| 1^+ | $\{cc\}_{1^3s_1}^{3c}$ | 3.14 | 3.226 | 3.16 | 3.22 | 3.30 | 3.329 |
| | $\{cc\}_{1^3d_1}^{3c}$ | 3.56 | 3.704 | 3.56 | | | |
| | $\{bb\}_{1^3s_1}^{3c}$ | 9.63 | 9.778 | 9.74 | 9.44 | 9.68 | 9.845 |
| | $\{bb\}_{1^3d_1}^{3c}$ | 10.02 | 10.123 | 10.08 | | | |
| | $\{bc\}_{1^3s_1}^{3c}$ | 6.42 | 6.526 | 6.48 | 6.35 | 6.50 | 6.611 |
| | $\{bc\}_{1^3d_1}^{3c}$ | 6.84 | | 6.85 | | | |
| 1^- | $\{cc\}_{1^1p_1}^{3c}$ | 3.41 | 3.460 | 3.39 | 3.42 | | |
| | $\{bb\}_{1^1p_1}^{3c}$ | 9.90 | 9.944 | 9.95 | 9.53 | | |
| | $\{bc\}_{1^1p_1}^{3c}$ | 6.65 | | 6.69 | 6.50 | | |

tetraquarks, is suitable for the doubly heavy diquarks.

We present a method to determine the parameters in the diquark Regge trajectories. Once the parameters are determined, the Regge trajectory becomes a new and very simple approach for estimating the spectra of diquarks. By employing (1) with (10) and (11) to fit the meson Regge trajectories, we can obtain values of the universal parameters. By fitting a chosen meson Regge trajectory, c_{0x} is calculated. After all parameters are computed, the diquark Regge trajectory is definite and

the spectra of diquarks can be estimated.

The diquark Regge trajectory is expected to provide a simple method to investigate easily the ρ -mode excitations of baryons, tetraquarks and pentaquarks in the diquark picture.

Acknowledgments

We are very grateful to the anonymous referees for the valuable comments and suggestions.

Appendix: States of diquarks

The diquark (qq') can be in two different $SU_c(3)$ configurations, $\bar{3}_c$ and 6_c . The diquark's color wave function is a superposition of these two different $SU_c(3)$ color representations [5, 80]:

$$\xi_{color} = a\xi_{\bar{3}_c} + b\xi_{6_c}, \quad a^2 + b^2 = 1. \quad (\text{A.1})$$

In the diquark picture, the diquark should be in $\bar{3}_c$ with a quark in 3_c to form a colorless baryon. In the tetraquark case, a diquark in $\bar{3}_c$ or in 6_c together with an antidiquark in 3_c or in $\bar{6}_c$ forms a color singlet.

The total wave function for the diquarks (qq') is written as

$$\psi_D = \xi_{color} \otimes \eta_{flavor} \otimes \chi_{spin} \otimes \phi_{space}, \quad (\text{A.2})$$

where ξ_{color} , η_{flavor} , χ_{spin} and ϕ_{space} are the color, flavor, spin and spatial wave functions, respectively, see Table VIII. If the quarks are of the same flavor $q = q'$, the diquark wave function ψ_D must be completely antisymmetric to satisfy the Pauli principle. When a diquark contains light quarks with flavors u,d,s, the overall state ψ_D must also be antisymmetric because strong interactions do not distinguish the flavor of u,d,s [11].

TABLE VIII: Wave functions are symmetric (S) or antisymmetric (A). The flavor wave function for the diquark (qq') can be symmetric $\{qq'\}$ or antisymmetric $[qq']$. s stands for the total spin of two quarks. $n = 0, 1, 2, \dots$.

| | ξ_{color} | η_{flavor} | χ_{spin} | ϕ_{space} |
|---|---------------|-----------------|---------------|----------------|
| S | 6_c | $\{qq'\}$ | $s = 1$ | $l = 2n$ |
| A | $\bar{3}_c$ | $[qq']$ | $s = 0$ | $l = 2n + 1$ |

In the color space, the color wave function can be analyzed by employing the $SU_c(3)$ group theory

$$3_c \otimes 3_c = \bar{3}_c \oplus 6_c. \quad (\text{A.3})$$

The color wave functions for the diquark read as

$$\xi_{\bar{3}_c} = |(qq')^{\bar{3}_c}\rangle, \quad \xi_{6_c} = |(qq')^{6_c}\rangle. \quad (\text{A.4})$$

The spin triplets are symmetric while the spin singlet is antisymmetric. The spin wave functions read as

$$\chi_S = |(qq')_1\rangle, \quad \chi_A = |(qq')_0\rangle. \quad (\text{A.5})$$

If $q \neq q'$, the flavor wave functions can be written in the symmetric and the antisymmetric form as

$$\begin{aligned} \eta_S = \{qq'\} &= \frac{1}{\sqrt{2}}(qq' + q'q), \\ \eta_A = [qq'] &= \frac{1}{\sqrt{2}}(qq' - q'q) \end{aligned} \quad (\text{A.6})$$

while

$$\eta_{flavor} = \eta_S = \{qq'\} = qq \quad (\text{A.7})$$

if $q = q'$.

Since quarks have the same intrinsic parities, the overall parity is

$$P((qq')) = (-1)^l, \quad (\text{A.8})$$

where l is the symmetry of the orbital wave function ϕ_{space} .

For the diquarks composed of two identical quarks, the antisymmetric flavor wave function does not exist; therefore, the states in the $[qq]$ configuration disappear in Table IX. From Table IX, we can easily read the possible mixing of different states. For example, for the diquarks composed of different quarks, the 1^+ state can be a mixture of the S-wave state and D-wave state, and the mixture of the $\bar{3}_c$ state and 6_c state.

-
- [1] M. Gell-Mann, Phys. Lett. **8**, 214-215 (1964)
 - [2] D. B. Lichtenberg and L. J. Tassie, Phys. Rev. **155**, 1601-1606 (1967)
 - [3] M. Anselmino, E. Predazzi, S. Ekelin, S. Fredriksson and D. B. Lichtenberg, Rev. Mod. Phys. **65**, 1199-1234 (1993)
 - [4] F. Wilczek, [arXiv:hep-ph/0409168 [hep-ph]].
 - [5] M. Y. Barabanov, M. A. Bedolla, W. K. Brooks, G. D. Cates, C. Chen, Y. Chen, E. Cisbani, M. Ding, G. Eichmann and R. Ent, *et al.* Prog. Part. Nucl. Phys. **116**, 103835 (2021) [arXiv:2008.07630 [hep-ph]].
 - [6] A. Selem and F. Wilczek, [arXiv:hep-ph/0602128 [hep-ph]].
 - [7] R. L. Jaffe and F. Wilczek, Phys. Rev. Lett. **91**, 232003 (2003) [arXiv:hep-ph/0307341 [hep-ph]].
 - [8] R. L. Jaffe, Phys. Rept. **409**, 1-45 (2005) [arXiv:hep-ph/0409065 [hep-ph]].
 - [9] M. Ida and R. Kobayashi, Prog. Theor. Phys. **36** (1966), 846
 - [10] Y. R. Liu, H. X. Chen, W. Chen, X. Liu and S. L. Zhu, Prog. Part. Nucl. Phys. **107** (2019), 237-320 [arXiv:1903.11976 [hep-ph]].
 - [11] A. Esposito, A. Pilloni and A. D. Polosa, Phys. Rept. **668** (2017), 1-97 [arXiv:1611.07920 [hep-ph]].
 - [12] R. L. Jaffe, Phys. Rev. D **15** (1977), 267
 - [13] R. F. Lebed, Phys. Lett. B **749** (2015), 454-457 [arXiv:1507.05867 [hep-ph]].
 - [14] S. L. Olsen, T. Skwarnicki and D. Zieminska, Rev. Mod. Phys. **90** (2018) no.1, 015003 [arXiv:1708.04012 [hep-ph]].
 - [15] F. K. Guo, X. H. Liu and S. Sakai, Prog. Part. Nucl.

TABLE IX: The completely antisymmetric states for the diquarks in $\bar{3}_c$ and in 6_c . j is the spin of the diquark (qq'), s denotes the total spin of two quarks, l represents the orbital angular momentum. $n = n_r + 1$, n_r is the radial quantum number, $n_r = 0, 1, 2, \dots$.

| Spin of diquark (j) | Parity (j^P) | Wave state ($n^{2s+1}l_j$) | Configuration |
|----------------------------|---------------------|---------------------------------|--|
| $j=0$ | 0^+ | n^1s_0 | $[qq']_{n^1s_0}^{3_c}, \{qq'\}_{n^1s_0}^{6_c}$ |
| | 0^- | n^3p_0 | $[qq']_{n^3p_0}^{3_c}, \{qq'\}_{n^3p_0}^{6_c}$ |
| $j=1$ | 1^+ | n^3s_1, n^3d_1 | $\{qq'\}_{n^3s_1}^{3_c}, \{qq'\}_{n^3d_1}^{3_c}, [qq']_{n^3s_1}^{6_c}, [qq']_{n^3d_1}^{6_c}$ |
| | 1^- | n^1p_1, n^3p_1 | $\{qq'\}_{n^1p_1}^{3_c}, [qq']_{n^3p_1}^{3_c}, [qq']_{n^1p_1}^{6_c}, \{qq'\}_{n^3p_1}^{6_c}$ |
| $j=2$ | 2^+ | n^1d_2, n^3d_2 | $[qq']_{n^1d_2}^{3_c}, \{qq'\}_{n^3d_2}^{3_c}, \{qq'\}_{n^1d_2}^{6_c}, [qq']_{n^3d_2}^{6_c}$ |
| | 2^- | n^3p_2, n^3f_2 | $[qq']_{n^3p_2}^{3_c}, [qq']_{n^3f_2}^{3_c}, \{qq'\}_{n^3p_2}^{6_c}, \{qq'\}_{n^3f_2}^{6_c}$ |
| \dots | \dots | \dots | \dots |

- Phys. **112** (2020), 103757 [arXiv:1912.07030 [hep-ph]].
- [16] S. S. Gershtein, V. V. Kiselev, A. K. Likhoded and A. I. Onishchenko, Phys. Rev. D **62**, 054021 (2000)
- [17] D. Ebert, R. N. Faustov, V. O. Galkin and A. P. Martynenko, Phys. Rev. D **66**, 014008 (2002) [arXiv:hep-ph/0201217 [hep-ph]].
- [18] L. X. Gutierrez-Guerrero, J. Alfaro and A. Raya, Int. J. Mod. Phys. A **36**, no.24, 2150171 (2021) [arXiv:2108.12532 [hep-ph]].
- [19] L. X. Gutierrez-Guerrero, G. Paredes-Torres and A. Bashir, Phys. Rev. D **104**, no.9, 094013 (2021) [arXiv:2109.09058 [hep-ph]].
- [20] P. L. Yin, Z. F. Cui, C. D. Roberts and J. Segovia, Eur. Phys. J. C **81**, no.4, 327 (2021) [arXiv:2102.12568 [hep-ph]].
- [21] Q. Li, C. H. Chang, S. X. Qin and G. L. Wang, Chin. Phys. C **44**, no.1, 013102 (2020) [arXiv:1903.02282 [hep-ph]].
- [22] Y. M. Yu, H. W. Ke, Y. B. Ding, X. H. Guo, H. Y. Jin, X. Q. Li, P. N. Shen and G. L. Wang, Commun. Theor. Phys. **46**, 1031-1039 (2006) [arXiv:hep-ph/0602077 [hep-ph]].
- [23] Z. G. Wang, S. L. Wan and W. M. Yang, Commun. Theor. Phys. **47**, 287-292 (2007) [arXiv:hep-ph/0506035 [hep-ph]].
- [24] R. T. Cahill, C. D. Roberts and J. Praschifka, Phys. Rev. D **36**, 2804 (1987)
- [25] P. Maris, Few Body Syst. **32**, 41-52 (2002) [arXiv:nucl-th/0204020 [nucl-th]].
- [26] Q. F. Lü, K. L. Wang, L. Y. Xiao and X. H. Zhong, Phys. Rev. D **96**, no.11, 114006 (2017) [arXiv:1708.04468 [hep-ph]].
- [27] J. Ferretti, Few Body Syst. **60**, no.1, 17 (2019)
- [28] M. Hess, F. Karsch, E. Laermann and I. Wetzorke, Phys. Rev. D **58**, 111502 (1998) [arXiv:hep-lat/9804023 [hep-lat]].
- [29] T. Regge, Nuovo Cim. **14**, 951 (1959)
- [30] G. F. Chew and S. C. Frautschi, Phys. Rev. Lett. **8**, 41 (1962)
- [31] C. Lovelace, Phys. Lett. **28B**, 264 (1968)
- [32] M. Ademollo, G. Veneziano and S. Weinberg, Phys. Rev. Lett. **22**, 83 (1969)
- [33] P. D. B. Collins, Phys. Rept. **1**, 103 (1971)
- [34] A. C. Irving and R. P. Worden, Phys. Rept. **34**, 117 (1977)
- [35] Y. Nambu, Phys. Lett. B **80**, 372 (1979)
- [36] S. Filipponi, Y. Srivastava, Phys. Rev. D **58**, 016003 (1998). arXiv:hep-ph/9712204
- [37] A. Inopin and G. S. Sharov, Phys. Rev. D **63**, 054023 (2001). arXiv: hep-ph/9905499.
- [38] M. M. Brisudova, L. Burakovsky and T. Goldman, Phys. Rev. D **61**, 054013 (2000). arXiv:hep-ph/9906293
- [39] A. V. Anisovich, V. V. Anisovich and A. V. Sarantsev, Phys. Rev. D **62**, 051502 (2000) [arXiv:hep-ph/0003113 [hep-ph]].
- [40] F. Brau, Phys. Rev. D **62**, 014005 (2000). arXiv:hep-ph/0412170
- [41] M. Baker and R. Steinke, Phys. Rev. D **65**, 094042 (2002). arXiv:hep-th/0201169
- [42] S. J. Brodsky, Eur. Phys. J. A **31**, 638 (2007). arXiv:hep-ph/0610115
- [43] H. Forkel, M. Beyer and T. Frederico, JHEP **0707**, 077 (2007). arXiv:hep-ph/0705.1857
- [44] X. H. Guo, K. W. Wei and X. H. Wu, Phys. Rev. D **78**, 056005 (2008). arXiv:hep-ph/0809.1702
- [45] D. Ebert, R. N. Faustov and V. O. Galkin, Phys. Rev. D **79**, 114029 (2009) [arXiv:0903.5183 [hep-ph]].
- [46] P. Masjuan, E. Ruiz Arriola and W. Broniowski, Phys. Rev. D **85**, 094006 (2012) [arXiv:1203.4782 [hep-ph]].
- [47] B. Chen, K. W. Wei and A. Zhang, Eur. Phys. J. A **51**, 82 (2015) [arXiv:1406.6561 [hep-ph]].
- [48] S. S. Afonin and I. V. Pusekov, Phys. Rev. D **90**, no.9, 094020 (2014) [arXiv:1411.2390 [hep-ph]].
- [49] J. Sonnenschein and D. Weissman, Eur. Phys. J. C **79**, no.4, 326 (2019) [arXiv:1812.01619 [hep-ph]].
- [50] A. M. Badalian and B. L. G. Bakker, Phys. Rev. D **100**, no.5, 054036 (2019) [arXiv:1902.09174 [hep-ph]].
- [51] M. A. Martin Contreras and A. Vega, Phys. Rev. D **102**, no.4, 046007 (2020) [arXiv:2004.10286 [hep-ph]].
- [52] J. K. Chen, Nucl. Phys. B **983**, 115911 (2022) [arXiv:2203.02981 [hep-ph]].
- [53] X. C. Feng and K. W. Wei, [arXiv:2303.10332 [hep-ph]].
- [54] J. K. Chen, [arXiv:2302.05926 [hep-ph]].
- [55] J. K. Chen, [arXiv:2302.06794 [hep-ph]].
- [56] The Regge trajectories are commonly plotted in the (M^2, x) plane or in the (x, M^2) plane, where $x = l, n_r$. For simplicity, the figures plotted in the (M, x) plane, in the $(M - m, x)$ plane and in the $((M - m)^2, x)$ plane are also called the Regge trajectories.
- [57] M. Baldicchi, A. V. Nesterenko, G. M. Prosperi, D. V. Shirkov and C. Simolo, Phys. Rev. Lett. **99** (2007), 242001 [arXiv:0705.0329 [hep-ph]].

- [58] M. Baldicchi, A. V. Nesterenko, G. M. Prosperi and C. Simolo, Phys. Rev. D **77** (2008), 034013 [arXiv:0705.1695 [hep-ph]].
- [59] N. Brambilla, E. Montaldi and G. M. Prosperi, Phys. Rev. D **54** (1996), 3506-3525 [arXiv:hep-ph/9504229 [hep-ph]].
- [60] J. K. Chen, Acta Phys. Pol. B **47**, 1155 (2016)
- [61] J. K. Chen, Rom. J. Phys. **62**, 119 (2017)
- [62] J. K. Chen, Eur. Phys. J. C **78**, no.3, 235 (2018)
- [63] J. K. Chen, Phys. Lett. B **786**, 477-484 (2018) [arXiv:1807.11003 [hep-ph]].
- [64] J. K. Chen, Eur. Phys. J. C **78** (2018) no.8, 648
- [65] J. K. Chen, Eur. Phys. J. A **57**, 238 (2021) [arXiv:2102.07993 [hep-ph]].
- [66] X. Z. Weng, W. Z. Deng and S. L. Zhu, Chin. Phys. C **46**, no.1, 013102 (2022) [arXiv:2108.07242 [hep-ph]].
- [67] M. Praszalowicz, Phys. Rev. D **106**, no.11, 114005 (2022) [arXiv:2208.08602 [hep-ph]].
- [68] E. Eichten, K. Gottfried, T. Kinoshita, J. B. Kogut, K. D. Lane and T. M. Yan, Phys. Rev. Lett. **34**, 369-372 (1975) [erratum: Phys. Rev. Lett. **36**, 1276 (1976)]
- [69] W. Lucha, F. F. Schoberl and D. Gromes, Phys. Rept. **200**, 127-240 (1991)
- [70] D. Gromes, Z. Phys. C **11**, 147 (1981)
- [71] F. Brau, Phys. Rev. D **62**, 014005 (2000) [arXiv:hep-ph/0412170 [hep-ph]].
- [72] S. Tomonaga, *Quantum Mechanics, Volume I: Old Quantum Theory* (North-Holland Publishing Company, Amsterdam, 1962)
- [73] I.S. Gradshteyn and I.M. Ryzhik, *Table of Integrals, Series, and Products*, corrected and, enlarged edition (Academic Press, New York, 1980)
- [74] R. L. Workman *et al.* [Particle Data Group], PTEP **2022** (2022), 083C01
- [75] J. Sonnenschein and D. Weissman, JHEP **08**, 013 (2014) [arXiv:1402.5603 [hep-ph]].
- [76] R. N. Faustov and V. O. Galkin, Phys. Rev. D **105**, no.1, 014013 (2022) [arXiv:2111.07702 [hep-ph]].
- [77] E. Eichten, S. Godfrey, H. Mahlke and J. L. Rosner, Rev. Mod. Phys. **80**, 1161-1193 (2008) [arXiv:hep-ph/0701208 [hep-ph]].
- [78] S. Godfrey, Phys. Rev. D **70**, 054017 (2004) [arXiv:hep-ph/0406228 [hep-ph]].
- [79] R. N. Faustov, V. O. Galkin and E. M. Savchenko, Phys. Rev. D **102**, no.11, 114030 (2020) [arXiv:2009.13237 [hep-ph]].
- [80] M. N. Anwar, J. Ferretti and E. Santopinto, Phys. Rev. D **98**, no.9, 094015 (2018) [arXiv:1805.06276 [hep-ph]].